

## Dimensional Crossover in the Purple Bronze $\text{Li}_{0.9}\text{Mo}_6\text{O}_{17}$

C. A. M. dos Santos,<sup>1,2</sup> B. D. White,<sup>1</sup> Yi-Kuo Yu,<sup>3</sup> J. J. Neumeier,<sup>1</sup> and J. A. Souza<sup>1</sup>

<sup>1</sup>Department of Physics, Montana State University, P. O. Box 173840, Bozeman, Montana 59717-3840, USA

<sup>2</sup>Escola de Engenharia de Lorena—USP, P. O. Box 116, Lorena, SP 12602-810, Brazil

<sup>3</sup>National Center for Biotechnology Information, 8600 Rockville Pike, Bethesda, Maryland 20894, USA

(Received 22 November 2006; published 28 June 2007)

Thermal expansion of  $\text{Li}_{0.9}\text{Mo}_6\text{O}_{17}$  is *a*-axis dominated which reduces the separation of the conducting chains at low temperature enhancing the interchain coupling. This destabilizes the Luttinger-liquid fixed point leading to an electronic charge- (or spin-) density wave dominated by Coulomb repulsion, as predicted by theories for Luttinger liquids.

DOI: [10.1103/PhysRevLett.98.266405](https://doi.org/10.1103/PhysRevLett.98.266405)

PACS numbers: 71.10.Pm, 65.40.De, 67.55.Hc, 71.45.Lr

Electrical transport in ordinary metals is usually well described by Fermi liquid theory which states that, in the presence of Coulomb interactions, the elementary excitations (quasiparticles) behave essentially like noninteracting electrons. In particular, the quasiparticle momentum distribution preserves the discontinuity at the Fermi surface. However, theoretical work by Luttinger [1] showed that this model breaks down for one-dimensional (1D) systems where even weak Coulomb interactions can cause strong perturbations. In a Luttinger liquid (LL) there is no discontinuity in the momentum distribution at the Fermi surface. Other key features are spin-charge separation and power-law dependence of the correlation functions [1]. The fundamental nature of these predictions has led to the search for a real example of a system possessing LL behavior [2–4]. Some candidates are carbon nanotubes [4] and inorganic compounds such as  $\text{NbSe}_3$  and  $\text{TaS}_3$  [5]. Compared to these, the purple bronze  $\text{Li}_{0.9}\text{Mo}_6\text{O}_{17}$  is unique as a 3D crystal with quasi-1D band structure and highly anisotropic metallic behavior above  $\sim 28$  K [2,3,6,7].

An important issue regarding  $\text{Li}_{0.9}\text{Mo}_6\text{O}_{17}$  is the cause of the crossover from metallic to semiconductorlike behavior [7–9] near  $T_M = 28$  K. Magnetic susceptibility reveals no long-range magnetic order at  $T_M$  [7,9], but a charge-density wave (CDW) might occur [8]. Related Mo compounds [10,11] are well-known CDW systems because structural distortions due to Peierls instabilities are observed through diffraction or thermal expansion experiments; herein this is referred to as a phonon-induced CDW. For  $\text{Li}_{0.9}\text{Mo}_6\text{O}_{17}$ , high-resolution x-ray diffraction reveals no phonon-induced CDW [12] and a difference of opinion exists in interpreting the photoemission data: in one case they are thought to support LL behavior [2], while in the other  $\text{Li}_{0.9}\text{Mo}_6\text{O}_{17}$  is classified as a 3D metal above  $T_M$  and a gap is observed below, consistent with CDW behavior [8]. Localization was invoked as a potential explanation for the upturn in electrical resistivity below  $T_M$  based on optical conductivity measurements which reveal a decrease near  $T_M$ , but no gap [7]. However, the addition of more disorder by doping Li with 30% and 40% K has little affect on the upturn [13]. Clearly, an understanding of the

crossover from metallic to semiconductorlike behavior does not exist.

This Letter reports the first high-resolution thermal expansion measurements of  $\text{Li}_{0.9}\text{Mo}_6\text{O}_{17}$ . A novel [14] fused quartz thermal expansion cell is employed. It can detect 0.1 Å changes in specimen length for a relative resolution of about  $10^{-8}$ , nearly 1000 times better than the highest resolution diffraction measurements. The thermal expansion is highly anisotropic, promoting one-dimensional behavior above  $T_M = 28$  K. The feature at  $T_M$  is very different from that typical for compounds exhibiting phonon-induced CDW transitions, where electron-phonon coupling leads to a sizable jump in the thermal expansion coefficient. These observations indicate that  $T_M$  represents a *crossover* in dimensionality which destabilizes the LL fixed point leading to a CDW dominated by electronic interactions, as suggested by LL theories [15,16].

Single crystals of  $\text{Li}_{0.9}\text{Mo}_6\text{O}_{17}$  were grown using a temperature-gradient flux method [17].  $\text{Li}_2\text{MoO}_4$ ,  $\text{MoO}_2$ , and  $\text{MoO}_3$  were weighed in a glove box, sealed in an evacuated 15 cm long quartz tube, held at 575 °C for 4 days and then reacted 10 days in a gradient of 10 °C/cm (490 and 640 °C at the tube ends). The tube was cooled to room temperature and opened. The mixture was immersed in hydrochloric acid for 3 days to separate the single crystals from the flux. The largest obtained crystal was  $3.0 \times 2.5 \times 0.5$  mm<sup>3</sup> (mass  $\sim 8.5$  mg) with purple and bronze colors depending on the optical orientation. X-ray powder diffractometry carried out with ground single crystals showed only Bragg reflections of monoclinic  $\text{Li}_{0.9}\text{Mo}_6\text{O}_{17}$  with lattice parameters  $a = 12.762$ ,  $b = 5.523$ ,  $c = 9.499$  Å, and  $\beta = 90.61^\circ$  [17,18]. The single crystals used for thermal expansion had dimensions  $2.538 \times 2.708 \times 0.523$  mm<sup>3</sup> (crystal A) and  $2.768 \times 2.167 \times 0.308$  mm<sup>3</sup> (crystal B). Crystal orientation was determined by Laue diffraction. Four-probe electrical resistance measurements were performed in the range  $300 > T > 0.4$  K along the *b* axis, the highest electrical conductivity axis [6,9].

Figure 1 displays the electrical resistance as a function of temperature  $R(T)$  for crystal A. As expected [7,9], a

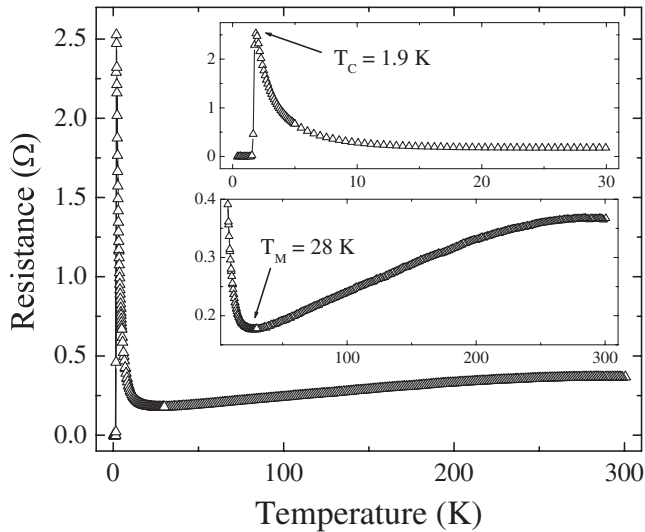


FIG. 1. Electrical resistance along the  $b$  axis (crystal A). Insets show the normal to superconducting transition and the metallic to semiconductorlike crossover.

crossover from metallic to semiconductorlike behavior is observed at  $T_M = 28$  K. The normal to superconducting phase transition at 1.9 K is highlighted in the upper inset. Similar results were obtained for crystal B. These aspects in  $R(T)$  are common to high-quality  $\text{Li}_{0.9}\text{Mo}_6\text{O}_{17}$  single crystals.

Linear thermal expansion normalized to the length at 300 K,  $\Delta L/L_{300}$ , for the  $a$ ,  $b$ , and  $c$  axes of crystal A is displayed in Fig. 2. These are raw data, corrected [14] only for the thermal expansion of quartz with no further processing. In spite of possible small variations in composition, the same behaviors are observed for crystal B indicating good reproducibility. The results reveal strong anisotropic behavior. The *in-plane* linear thermal expansions ( $b$  and  $c$  axes) display small linear thermal expansions, which are about 1 order of magnitude smaller than that of the  $a$  axis, revealing the layered character. Along the  $c$  axis the crystal contracts from room temperature to 220 K followed by an expansion with further cooling [see inset of Fig. 2(a)]. This behavior may be related to the curvature in  $R(T)$  above 200 K (see Fig. 1). Figure 2(b) highlights the  $b$  axis  $\Delta L/L_{300}$  for crystals A and B (inset) below 100 K. A maximum is evident at  $\sim 20$  K and a minimum occurs at  $\sim 60$  K; such behavior is not unusual for layered systems where negative thermal expansions (i.e., contraction upon warming) are generally associated with strongly anharmonic planar lattice vibrations [19]. This anomalous phonon behavior could be further investigated with spectroscopic methods. The bar in Fig. 2(b) provides an *absolute* scale for our measurements. For instance, the size of the peak below 28 K corresponds to a 20 Å length change of the 2.708 mm long sample, requiring relative resolution better than  $10^{-6}$ ; in fact, our resolution is 100 times higher.

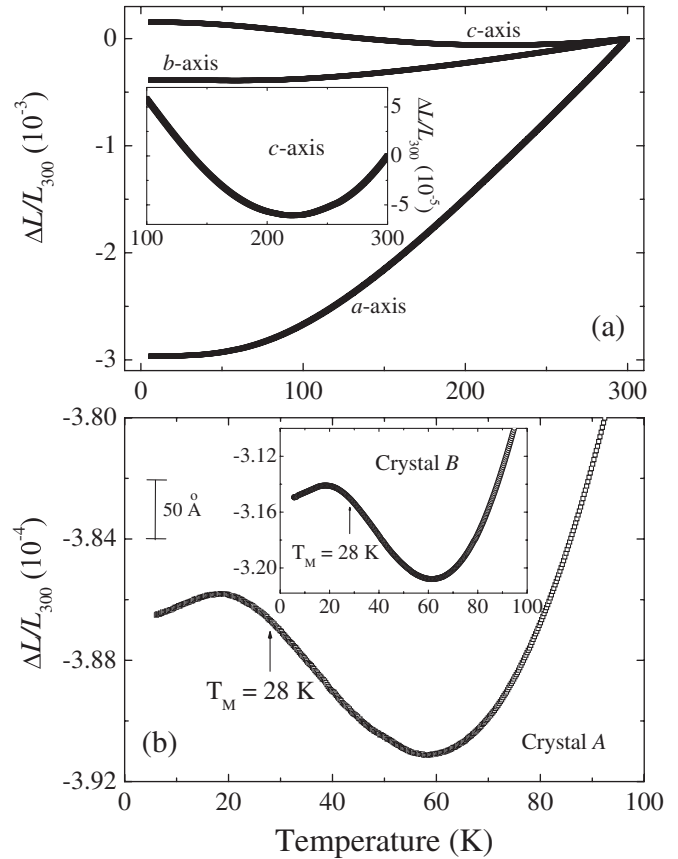


FIG. 2. (a) Linear thermal expansion  $\Delta L/L_{300}$  for  $a$ ,  $b$ , and  $c$  axes of crystal A. Inset highlights behavior of the  $c$  axis. (b)  $\Delta L/L_{300}$  along the  $b$  axis for crystals A and B (inset); 50 Å bar provides *absolute* scale.

Figure 3(a) displays the linear thermal expansion coefficients,  $\mu_i = d(\Delta L/L_{300})/dT$  for the  $i = a$ ,  $b$ , and  $c$  directions of crystal A, obtained following the procedure reported previously [14]. The volumetric thermal expansion coefficient [Fig. 3(a)] was calculated via  $\Omega = \mu_a + \mu_b + \mu_c$ ; the region near 28 K is highlighted in the inset revealing a distinct minimum near  $T_M$ . We note that this anomaly must be of the same origin as the small, broad peak observed in our (not shown) and reported heat capacity measurements [7,20]. Changes in the slope of  $\mu_i$  are evident in *all three* crystallographic directions near 28 K, as illustrated in Fig. 3(b). This is the first time that distinct features have been reported in a physical property of  $\text{Li}_{0.9}\text{Mo}_6\text{O}_{17}$  near  $T_M$ , a tribute to the high resolution of our measurements.

The character of the features near  $T_M$  in Fig. 3 is an important aspect of our observations. For continuous phase transitions, either a peak, jump, or cusp in susceptibilities such as  $\mu_i$  and  $\Omega$  will appear. The soft transformation of slopes in the data of Fig. 3 underscores the subtle changes in  $\mu_i$  and  $\Omega$  near  $T_M$ ; this leads us to identify it as a crossover of purely electronic nature. Furthermore, the features in Fig. 3 near  $T_M$  differ markedly from those observed in well-known phonon-induced CDW systems

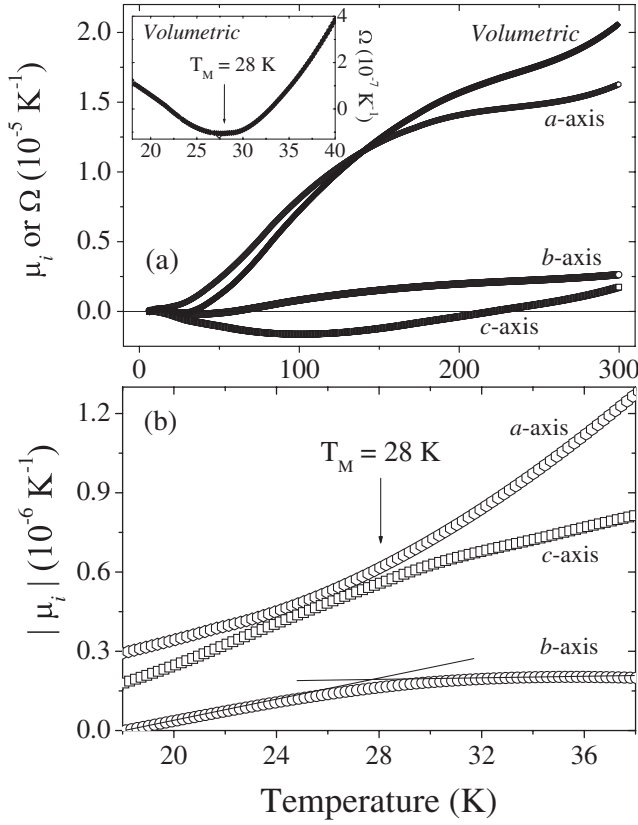


FIG. 3. Linear thermal expansion coefficient  $\mu_i$  and the volumetric thermal expansion coefficient  $\Omega$ . Inset highlights  $\Omega$  near  $T_M$ . (b) Absolute value of  $\mu_i$  near  $T_M$ ,  $\mu_b$  and  $\mu_c$  are negative in this region. Solid lines guide the eye.

such as  $\text{K}_{0.3}\text{MoO}_3$  [10,11], where sizable jumps in  $\mu_i$ ,  $\Omega$ , and heat capacity occur. The absence of such characteristic behavior leads us to conclude that the upturn in the electrical resistivity at  $T_M$  is *not* the result of a phonon-induced CDW transition. However, the possibility remains that the crossover is due to a CDW [or spin-density wave (SDW)] induced by Coulomb repulsion [15,16], a scenario of special importance in LL physics.

To better understand the thermal expansion of  $\text{Li}_{0.9}\text{Mo}_6\text{O}_{17}$  and its importance for the 28 K crossover from metallic to semiconductorlike behavior, the impact of  $\Delta L/L_{300}$  on the dimensionality is evaluated. The highest conductivity direction in  $\text{Li}_{0.9}\text{Mo}_6\text{O}_{17}$  is along the  $b$  axis through the Mo(1)-O(11)-Mo(4) parallel zigzag chains [3,18]. Clearly, the strong relative thermal expansion along  $a$  (Figs. 2 and 3) will affect the spacing between the zigzag chains. These chains are connected by O(1) atoms through Mo(1)-O(1)-Mo(4) bonds lying in the  $[\bar{1}02]$  crystallographic direction [3,18]. It is plausible that a reduction in the chain separation (i.e., a shrinkage along the  $[\bar{1}02]$  direction) that is *greater* than the reductions in length along the  $b$  and  $c$  axes may facilitate a change in the 1D behavior. Using our thermal expansion data for  $a$  and  $c$ , the linear thermal expansion coefficient for the  $[\bar{1}02]$  direction is calculated. Results at temperatures below 150 K are com-

pared with  $\mu_b$  (since it has the larger  $\mu_i$  of  $b$  or  $c$ ) in Fig. 4. At high temperatures the contraction along  $[\bar{1}02]$  is higher than the  $b$ -axis contraction. However, below  $\sim 30$  K these thermal expansion coefficients become comparable not only in magnitude, but also in behavior. Thus, we believe that the anisotropic thermal expansion coefficients *above* 28 K promote a reduction in the coupling between the neighboring Mo(1)-O(11)-Mo(4) zigzag chains, which are the one-dimensional conductivity channel. This observation substantiates our identification of  $T_M = 28$  K as a crossover temperature; below this temperature, the zigzag chains possess more interchain electronic coupling than above. We emphasize that quasi-1D behavior is documented at high temperature [9] and 3D behavior (superconductivity) occurs below 1.9 K. Thus, the issue is not *whether* a dimensionality crossover exists, but rather *at what temperature* it occurs.

From the theoretical point of view, it is well known that the LL fixed point may lose its stability against various generic perturbations. For example, low frequency phonons, when strongly coupled to the electrons, open a spin gap destabilizing the LL fixed point [1]. When  $0 < \alpha < 1$ , as observed in  $\text{Li}_{0.9}\text{Mo}_6\text{O}_{17}$  [6], there exists another instability towards higher-dimensional behavior. At a temperature below the crossover temperature  $T_{1D} \sim (t_{\perp})^{1/(1-\alpha)}$ , depending on the  $\alpha$  value, the LL fixed point may be destabilized via single-fermion hopping (for smaller  $\alpha$ ) or two-fermion hopping (for larger  $\alpha$ ). The former leads to a Fermi liquid [15,21,22], while the latter leads to semiconductor CDW or SDW (hereafter referred to as CDW/SDW) behavior provided that the electron-electron interaction is repulsive and singlet or triplet superconducting states if it is attractive [15].

For the purple bronze analyzed in the context of LL theory,  $\alpha$  lies in the range  $0.5 < \alpha < 0.9$  [2,6]. Thus, it is likely that the dimensional crossover is governed by two-

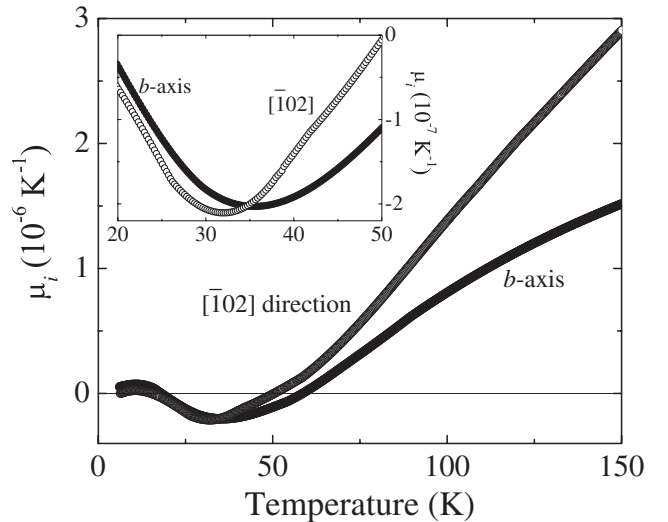


FIG. 4. Behavior of the linear thermal coefficients for  $b$  axis and the  $[\bar{1}02]$  direction. Inset highlights region near 28 K.

fermion hopping leading to insulator or semiconductorlike behavior due to CDW/SDW formation; unlike typical phonon-induced CDW/SDWs, this one is dominated by electronic interactions [15,16]. Furthermore, the small, broad features in the heat capacity [7,20] and  $\Omega$  indicate a small entropy change, one that is likely electronic in origin. Analysis of photoemission data [8] suggests a CDW scenario; however, we remark on the observed energy gap and classification of the purple bronze as a 3D Fermi liquid [8] for  $T > T_M$ . Although the observation of a gap at low temperature (17 K) is convincing, it is about 60 times larger than suggested by our  $R(T)$  data [23]. Furthermore, the intensity versus binding energy for low-lying excitation states along the quasi-1D direction reveals no peak that is distinct from the background, contradicting what is expected for a normal Fermi liquid [24]. In addition, recent experiments fail to observe a gap at low temperature and are consistent with LL physics [2,6]. Therefore, it remains unclear as to whether  $\text{Li}_{0.9}\text{Mo}_6\text{O}_{17}$  is truly a LL or just a Fermi liquid at  $T > T_M$ . Nonetheless, based on our results, if at  $T > T_M$  the system indeed follows LL behavior, then it most likely will crossover near  $T_M$  to a CDW/SDW [15]. Not only is this consistent with the observed upturn in the electrical resistivity at  $T < T_M$ , the dimensionality crossover may also set the stage for superconductivity occurring at 1.9 K, a 3D phenomenon.

In summary, changes in interchain spacing of  $\text{Li}_{0.9}\text{Mo}_6\text{O}_{17}$  that could facilitate the crossover in dimensionality have been revealed. This and the subtle nature of the feature in the thermal expansion coefficients near  $T_M$  lead us to identify this temperature as the dimensionality crossover temperature  $T_{1D}$  predicted in LL theories when the anomalous exponent  $\alpha$  is small ( $0 < \alpha < 1$ ) [15]. These considerations suggest development of a CDW/SDW below  $T_M$  that is mostly electronic in nature; this would explain the subtle features in  $\mu_i$ ,  $\Omega$ , and heat capacity near  $T_M$ , compared to related phonon-induced CDW systems, and is consistent with the upturn in the electrical resistivity below  $T_M$ .

The authors thank J.V. Alvarez and J.W. Allen for encouragement to undertake this study and H.J. Izário Filho and A.J.S. Machado for chemical analysis of the crystals. This material is based upon work supported by the National Science Foundation (No. DMR-0504769), U.S. Department of Energy Office of Basic Energy Sciences (No. DE-FG-06ER46269), and Brazilian agencies CAPES (No. 0466/05-0) and CNPq (No. 201017/2005-9). This work was partially supported by the Intramural Research Program of the National Library of Medicine at the NIH.

- 
- [1] J. Voit, Rep. Prog. Phys. **58**, 977 (1995).  
 [2] F. Wang, J.V. Alvarez, S.-K. Mo, J.W. Allen, G.-H. Gweon, J. He, R. Jin, D. Mandrus, and H. Höchst, Phys. Rev. Lett. **96**, 196403 (2006); G.-H. Gweon, S.-K. Mo,

- J.W. Allen, J. He, R. Jin, D. Mandrus, and H. Höchst, Phys. Rev. B **70**, 153103 (2004).  
 [3] Z.S. Popović and S. Satpathy, Phys. Rev. B **74**, 045117 (2006).  
 [4] R. Tarkiainen, M. Ahlskog, J. Penttilä, L. Roschier, P. Hakonen, M. Paalanen, and E. Sonin, Phys. Rev. B **64**, 195412 (2001).  
 [5] S.N. Artemenko and S.V. Remizov, Phys. Rev. B **72**, 125118 (2005); S.V. Zaitsev-Zotov, M.S.H. Go, E. Slot, and H.S.J. van der Zant, Phys. Low-Dim. Struct. **1-2**, 79 (2002).  
 [6] J. Hager, R. Matzdorf, J. He, R. Jin, D. Mandrus, M.A. Cazalilla, and E.W. Plummer, Phys. Rev. Lett. **95**, 186402 (2005).  
 [7] J. Choi, J.L. Musfeldt, J. He, R. Jin, J.R. Thompson, D. Mandrus, X.N. Lin, V.A. Bondarenko, and J.W. Brill, Phys. Rev. B **69**, 085120 (2004).  
 [8] K.E. Smith, K. Breuer, M. Greenblatt, and W. McCarroll, Phys. Rev. Lett. **70**, 3772 (1993); J. Xue, L.-C. Duda, K.E. Smith, A.V. Fedorov, P.D. Johnson, S.L. Hulbert, W. McCarroll, and M. Greenblatt, *ibid.* **83**, 1235 (1999).  
 [9] M. Greenblatt, Chem. Rev. **88**, 31 (1988).  
 [10] J.W. Brill, M. Chung, Y.-K. Kuo, X. Zhan, E. Figueroa, and G. Mozurkewich, Phys. Rev. Lett. **74**, 1182 (1995).  
 [11] M.R. Hauser, B.B. Plapp, and G. Mozurkewich, Phys. Rev. B **43**, 8105 (1991); A.H. Moudden, M. Elmiger, S.M. Shapiro, B.T. Collins, and M. Greenblatt, *ibid.* **44**, 3324 (1991); H. Negishi, Y. Kuroiwa, H. Akamine, S. Aoyagi, A. Sawada, T. Shobu, S. Negishi, and M. Sasaki, Solid State Commun. **125**, 45 (2003).  
 [12] J.-P. Pouget (private communication).  
 [13] Y. Matsuda, M. Sato, M. Onoda, and K. Nakao, J. Phys. C **19**, 6039 (1986).  
 [14] J.J. Neumeier, T. Tomita, M. Debessai, J.S. Schilling, P.W. Barnes, D.G. Hinks, and J.D. Jorgensen, Phys. Rev. B **72**, 220505 (2005).  
 [15] D. Boies, C. Bourbonnais, and A.-M.S. Tremblay, Phys. Rev. Lett. **74**, 968 (1995).  
 [16] A phonon-induced CDW originates from electron-phonon coupling; the electron's kinetic energy is lowered at the expense of elastic energy. A purely electronic CDW is specific to quasi-1D systems. It originates from Coulomb repulsion which can lead to backscattering and mixing of electrons; this causes the CDW. No appreciable lattice distortion is expected since phonons, although present, play a minor role.  
 [17] W.H. McCarroll and M. Greenblatt, J. Solid State Chem. **54**, 282 (1984).  
 [18] M. Onoda, K. Toriumi, Y. Matsuda, and M. Sato, J. Solid State Chem. **66**, 163 (1987).  
 [19] N.A. Abdullaev, Phys. Solid State **43**, 727 (2001).  
 [20] C. Schlenker, J. Dumas, C. Escribe-Filippini, H. Guoy, J. Marcus, and G. Fourcaudot, Philos. Mag. B **52**, 643 (1985).  
 [21] X.G. Wen, Phys. Rev. B **42**, 6623 (1990).  
 [22] Summing the leading-logarithmic divergence to all orders,  $\alpha$  scales to zero below the crossover temperature; see E. Arrigoni, Phys. Rev. Lett. **83**, 128 (1999).  
 [23] Electrical resistivity below 28 K ( $\log[R(T)]$  vs  $1/T$ ) is nonlinear. A crude linear fit in the narrow range  $6 < T < 17$  K gives an estimate of 1.3 meV for the gap.  
 [24] G.A. Sawatzky, Nature (London) **342**, 480 (1989).